TÜBİTAK

Turkish Journal of Physics

http://journals.tubitak.gov.tr/physics/

Research Article

Turk J Phys
(2016) 40: 40 – 51

doi:10.3906/fiz-1508-21

Effects of variable viscosity and thermal conductivity on magnetohydrodynamic free convection flow of a micropolar fluid past a stretching plate through porous medium with radiation, heat generation, and Joule dissipation

Gopal Chandra HAZARIKA[1,*], **Bandita PHUKAN**[1,2]
[1]Department of Mathematics, Faculty of Mathematics, Dibrugarh University, Dibrugarh, India
[2]Department of Mathematics, Dibrugarh University, Dibrugarh, India

Received: 27.08.2015 • **Accepted/Published Online:** 31.01.2016 • **Final Version:** 12.02.2016

Abstract: The effects of temperature-dependent viscosity and thermal conductivity on free convection magnetohydrodynamic flow of an optically thin gray, viscous, and incompressible micropolar fluid and heat transfer past a stretching plate through porous medium in the presence of radiation, heat generation, and Joule dissipation were studied. The fluid viscosity and thermal conductivity were assumed to vary as inverse linear functions of temperature. Using similarity transformation, the governing partial differential equations of motion were reduced to ordinary ones, which were solved numerically for prescribed boundary conditions using the shooting method. Numerical results for the velocity, angular velocity, and temperature profiles are shown graphically and the skin friction and Nusselt number are presented in tabular form for various values of the parameters, giving the flow and heat transfer characteristics. We found that viscosity enhanced microrotation, while an increase in thermal conductivity reduced the temperature.

Key words: Magnetohydrodynamic, micropolar fluid, optically thin gray fluid, shooting method, radiation

1. Introduction

Micropolar fluids containing microconstituents that can undergo rotation can be defined as viscous non-Newtonian fluids with nonsymmetrical stress tensor. In micropolar fluid theory the presence of a microstructure and the intrinsic motion of the fluid elements affect the hydrodynamics of the flow.

The study of micropolar fluid flow and heat transfer is important as it has many engineering applications such as polymer processing, micro fluidics, oil exploration, geothermal extractions, and coating. Accordingly, the effects of radiation on magnetohydrodynamics (MHD) are of considerable interest because of their increasing practical application in fields such as space technology and high temperature plasmas.

Keeping in view the wide area of practical importance, the theory of micropolar fluid, developed by Eringen [1] has become a field of active research for the past few decades. Numerical investigation on heat and mass transfer effects of micropolar fluid over a stretching sheet through porous media was done by Mohanty et al. [2]. An analytic solution to the micropolar fluid flow through a semiporous channel with an expanding or contracting wall was determined by Si et al. [3]. Ashraf and Batool [4] investigated the MHD flow and heat transfer of a micropolar fluid over a stretchable disk. Si et al. [5] studied the flow and heat transfer of a micropolar fluid in a porous channel with expanding or contracting walls. Raptis and Perdikis [6] studied the free convective oscillatory flow and heat mass transfer past a porous plate in the presence of radiation

*Correspondence: gchazarika@gmail.com

for an optically thin fluid. Siddheshwar and Mahabaleshwar [7] examined the analytical solution to the MHD flow of micropolar fluid over a linear stretching sheet. The MHD effects on thin films of unsteady micropolar fluid through a porous medium were investigated by Rahman [8]. Khedr et al. [9] discussed the MHD flow of a micropolar fluid past a stretched permeable surface with heat generation or absorption. The effects of variable viscosity and thermal conductivity on the hydromagnetic boundary layer micropolar fluid flow over a stretching surface embedded in a non-Darcian porous medium with radiation sheet were analyzed by Borgohain and Hazarika [10]. Raptis [11] examined the thermal radiation of an optically thin gray gas. The radiation effects on flow past a stretching plate of an optically thin gray viscous fluid with temperature-dependent viscosity were analyzed by Xenos [12].

In most previous studies the physical properties of the micropolar fluid were assumed to be constant, including or excluding MHD effects for various geometries. However, as no work has been conducted on the effects of variable viscosity and thermal conductivity on MHD free convection flow of a micropolar fluid with radiation, we investigated the effects of temperature-dependent viscosity and thermal conductivity on free convection MHD flow and heat transfer of a micropolar fluid past a stretching plate through porous medium in the presence of radiation, heat generation, and Joule dissipation. The fluid viscosity and thermal conductivity are assumed to vary as inverse linear functions of temperature. Using similarity transformation, the governing partial differential equations of motion are reduced to ordinary differential equations, which are solved numerically for prescribed boundary conditions using the shooting method.

2. Mathematical formulation of the problem

We consider the steady two-dimensional flow of a viscous incompressible micropolar fluid past a stretching plate through a porous medium. Let (u,v) be the velocity component along (x,y) direction, where the x-axis is taken along the plate and the y-axis is considered normal to the x-axis, as shown in Figure 1. The plate is stretched by introducing two equal and opposite forces so that the position of the plate remain the same. A transverse uniform magnetic field B_0 acts on the plate. The fluid properties are assumed to be isotropic and constant, except for the fluid viscosity and thermal conductivity, which are assumed to be inverse linear functions of temperature. The radiation heat flux in the x-direction is considered negligible in comparison with that in the y-direction. Let N be the microrotation component.

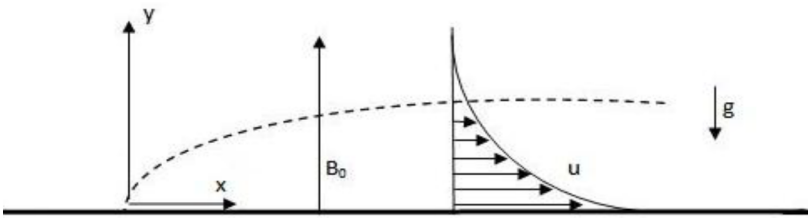

Figure 1. Flow configuration.

Under the boundary layer assumptions, the governing equations of motion are given below:
The equation of continuity:

$$\frac{\partial u}{\partial x} + \frac{\partial v}{\partial y} = 0 \tag{1}$$

The momentum equation:

$$u\frac{\partial u}{\partial x}+v\frac{\partial u}{\partial y}=\frac{1}{\rho}\left(\frac{\partial \mu}{\partial y}\frac{\partial u}{\partial y}+\mu\frac{\partial^2 u}{\partial y^2}\right)+\frac{\kappa}{\rho}\left(\frac{\partial^2 u}{\partial y^2}+\frac{\partial N}{\partial y}\right)-\frac{\sigma B_0^2 u}{\rho}+g\beta\left(T-T_\infty\right)-\frac{\nu}{m^*}u \tag{2}$$

The angular momentum equation:

$$\rho j\left(u\frac{\partial N}{\partial x}+v\frac{\partial N}{\partial y}\right)=-\kappa\left(2N+\frac{\partial u}{\partial y}\right)+\gamma\frac{\partial^2 N}{\partial y^2} \tag{3}$$

The energy equation:

$$\rho C_p\left(u\frac{\partial T}{\partial x}+v\frac{\partial T}{\partial y}\right)=\frac{\partial \lambda}{\partial y}\frac{\partial T}{\partial y}+\lambda\frac{\partial^2 T}{\partial y^2}+(\mu+\kappa)\left(\frac{\partial u}{\partial y}\right)^2-\frac{\partial q_r}{\partial y}+\sigma(uB_0)^2+Q_0(T-T_\infty) \tag{4}$$

The boundary conditions are:

$$\left.\begin{aligned} &u=cx, v=0, T=T_w, N=-\frac{1}{2}\frac{\partial u}{\partial y} \text{ at } y=0\\ &u\to 0, T\to T_\infty, N\to 0 \text{ as } y\to\infty \end{aligned}\right\} \tag{5}$$

where ρ is the fluid density, μ is the coefficient of dynamic viscosity, T is the fluid temperature, λ is the thermal conductivity, m^* is the coefficient of permeability, j is the microinertia per unit mass, C_p is the specific heat at constant pressure, σ is the electrical conductivity, γ and κ are material parameters, q_r is the radiative heat flux, g is the acceleration due to gravity, β is the coefficient of thermal expansion, Q_0 is the heat generation coefficient, and c is a constant.

Following Lai and Kulacki [13], the fluid viscosity is assumed as:

$$\left.\begin{aligned} &\frac{1}{\mu}=\frac{1}{\mu_\infty}[1+\delta(T-T_\infty)]\\ &\text{or, } \frac{1}{\mu}=a(T-T_r)\\ &\text{where } a=\frac{\delta}{\mu_\infty} \text{ and } T_r=T_\infty-\frac{1}{\delta} \end{aligned}\right\} \tag{6}$$

where μ_∞ is the viscosity at infinity, and a and T_∞ are constants and their values depend on the reference state and thermal property of the fluid. T_r is transformed reference temperature related to the viscosity parameter, δ is a constant based on the thermal property of the fluid, and $a<0$ for gas, $a>0$ for liquid.

Similarly, the thermal conductivity is considered as:

$$\left.\begin{aligned} &\frac{1}{\lambda}=\frac{1}{\lambda_\infty}[1+\xi(T-T_\infty)]\\ &\frac{1}{\lambda}=b(T-T_k)\\ &b=\frac{\xi}{\lambda_\infty}, \text{ and } T_k=T_\infty-\frac{1}{\xi} \end{aligned}\right\} \tag{7}$$

where b and T_k are constants and their values depend on the reference state and thermal properties of the fluid, i.e. on ξ.

For the case of an optically thin gray fluid, the local radiant is given by Xenos [12] as:

$$-\frac{\partial q_r}{\partial y} = 4a^*\sigma^*\left(T_\infty^4 - T^4\right) \tag{8}$$

where a^* is the absorption coefficient and σ^* is the Stefan–Boltzmann constant. It is assumed that the temperature differences within the flow are sufficiently small so that T^4 may be expressed as a linear function of the temperature and can be expanded in Taylor series about T_∞, which, after neglecting higher order terms, takes the following form:

$$T^4 \cong 4T_\infty^3 T - 3T_\infty^4 \tag{9}$$

Using Eqs. (9) and (8), Eq. (4) can be rewritten as:

$$\rho C_p\left(u\frac{\partial T}{\partial x} + v\frac{\partial T}{\partial y}\right) = \frac{\partial \lambda}{\partial y}\frac{\partial T}{\partial y} + \lambda\frac{\partial^2 T}{\partial y^2} + (\mu+\kappa)\left(\frac{\partial u}{\partial y}\right)^2 + 16a^*\sigma^*T_\infty^3(T_\infty - T) + \sigma(uB_0)^2 + Q_0(T - T_\infty) \tag{10}$$

Let us introduce the following similarity transformations and parameters:

$$\left.\begin{aligned} &u = cxf'(\eta), \quad \eta = y\left(\frac{c}{\nu_\infty}\right)^{\frac{1}{2}} \\ &v = -\left(\nu_\infty c\right)^{\frac{1}{2}} f(\eta) \\ &\theta = \frac{T - T_\infty}{T_w - T_\infty}, \quad N = cx\left(\frac{c}{\nu_\infty}\right)^{\frac{1}{2}} g(\eta) \end{aligned}\right\} \tag{11}$$

Using the above transformations, the equation of continuity (1) is satisfied identically and Eqs. (2), (3), and (10) are respectively reduced to canonical form as the following:

$$f''' = \frac{1}{1 - K\left(\frac{\theta-\theta_r}{\theta_r}\right)}\left[\left(\frac{\theta-\theta_r}{\theta_r}\right)(ff'' - f'^2 + Kg') + \frac{\theta' f''}{\theta - \theta_r} + \left(\frac{M^2}{Re}f' + \frac{Gr}{Re^2}\theta\right)\left(\frac{\theta-\theta_r}{\theta_r}\right) + \frac{f'}{mRe}\right] \tag{12}$$

$$g'' = \frac{1}{G}(2g + f'') + \frac{1}{\Delta}(f'g - fg') \tag{13}$$

$$\theta'' = \frac{\theta'^2}{(\theta - \theta_k)} + \Pr\left(\frac{\theta-\theta_k}{\theta_k}\right) f\theta' + \Pr Ec\left(K - \frac{\theta_r}{\theta - \theta_r}\right)\left(\frac{\theta-\theta_k}{\theta_k}\right) f''^2 + (\Pr Q - S)\theta\left(\frac{\theta-\theta_k}{\theta_k}\right) \tag{14}$$

where

$$\theta_r = \frac{T_r - T_\infty}{T_w - T_\infty} = \frac{1}{\delta\left(T_w - T_\infty\right)} \text{ and } \theta_k = \frac{T_k - T_\infty}{T_w - T_\infty} = \frac{1}{\xi\left(T_w - T_\infty\right)}$$

are dimensionless reference temperatures corresponding to viscosity and thermal conductivity, respectively. It is to be noted that these values are negative for liquids and positive for gases when $(T_w - T_\infty)$ is positive (Lai and Kulacki [13]).

Here the dimensionless parameters are defined as:

$Re = \frac{cx^2}{\nu_\infty}$ is the stretching Reynolds number;

$G = \frac{c\gamma}{\kappa\nu_\infty}$ is the microrotation parameter;

$K = \frac{\kappa}{\mu_\infty}$ is the coupling constant parameter;

$\Delta = \frac{\gamma}{\mu_\infty j}$ is the material constant;

$M = \left(\frac{\sigma}{\mu_\infty}\right)^{\frac{1}{2}} B_0 x$ is the Hartmann number;

$m = \frac{m^*}{x^2}$ is the permeability number;

$\Pr = \frac{\mu_\infty C_p}{\lambda_\infty}$ is the Prandtl number;

$Ec = \frac{c^2 x^2}{C_p(T_w - T_\infty)}$ is the Eckert number;

$S = \frac{16a^*\sigma^* T_\infty^3 \nu_\infty}{c\lambda_\infty}$ is the radiation parameter;

$Q = \frac{Q_0}{c\rho C_p}$ is the heat generation parameter; and

$Gr = \frac{g\beta(T_w - T_\infty)x^3}{\nu_\infty^2}$ is the Grashof number.

The boundary conditions (6) are reduced to:

$$\left.\begin{array}{l} \text{at } \eta = 0, f = 0, f' = 1, \theta = 1, g = -\dfrac{1}{2} f'' \\ \text{as } \eta \to \infty, f' \to 0, \theta \to 0, g \to 0 \end{array}\right\} \tag{15}$$

The important physical quantities of interest in this problem are the skin friction coefficient C_f and the Nusselt number Nu, which represent the rate of plate shear stress and the rate of heat transfer from the surface, respectively. These are defined as:

$$C_f = \frac{2\tau_w}{\rho_\infty U_0^2},$$

where τ_w is the shear stress which is given by:

$$\tau_w = \left[(\mu + \kappa)\frac{\partial u}{\partial y} + \kappa N\right]_{y=0}$$

and $Nu = \frac{x q_w}{\lambda_\infty (T_w - T_\infty)}$

where q_w is the heat transfer from the surface given by:

$$q_w = -\left(\lambda \frac{\partial T}{\partial y}\right)_{y=0}$$

Thus, $C_f Re^{\frac{1}{2}} = (\frac{2\theta_r}{\theta_r - 1} + K) f''(0)$ and $NuRe^{-\frac{1}{2}} = -\frac{\theta_k}{\theta_k - 1}\theta'(0)$.

3. Results and discussion

The systems of differential equations (Eqs. (12)–(14)), together with the boundary conditions (Eq. (15)), are solved numerically by applying the shooting method, an efficient numerical technique in conjunction with the forth order Runge–Kutta method, which is solved by developing suitable codes for MATLAB. The numerical values of different parameters are taken as Re = 0.1, M = 0.5, Pr = 0.7, Ec = 0.01, $\theta_r = -10$, $\theta_k = -10$, G = 1, $\Delta = 0.5$, K = 0.1, m = 0.25, S = 0.5, Q = 1, and Gr = 0.1 unless stated otherwise.

The variations in velocity profile, microrotation profile, and temperature profile are presented in Figures 2–17 for the variations of different parameters involved in the equations. Variations in the velocity profile are shown in Figures 2–7. From Figures 2, 4, 5, 6, and 7 it is clear that velocity decreases with the increase of the viscosity parameter θ_r, the heat generation parameter Q, and the Grashof number Gr, whereas it increases as the values of the radiation parameter S and the coupling constant parameter K increase. Due to the increase in viscous and buoyancy force and the generation of heat during the flow, velocity decreases. For small values of the coupling constant parameter, the viscous force is predominant and as a result viscosity increases, and therefore velocity decreases. Figure 3 shows that there is no significant variation in velocity with the thermal conductivity parameter θ_k.

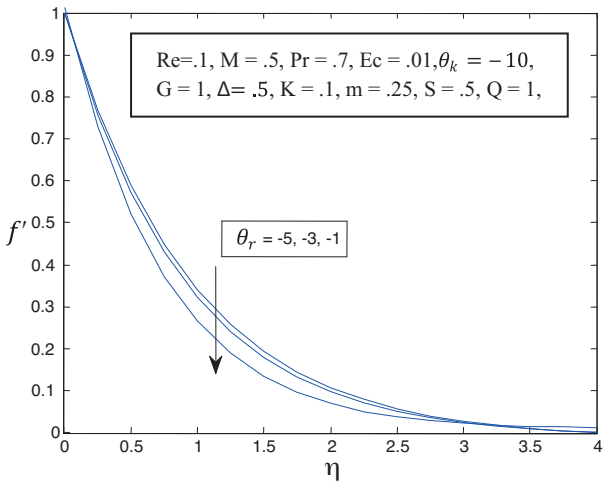

Figure 2. Velocity profile for different values of θ_r

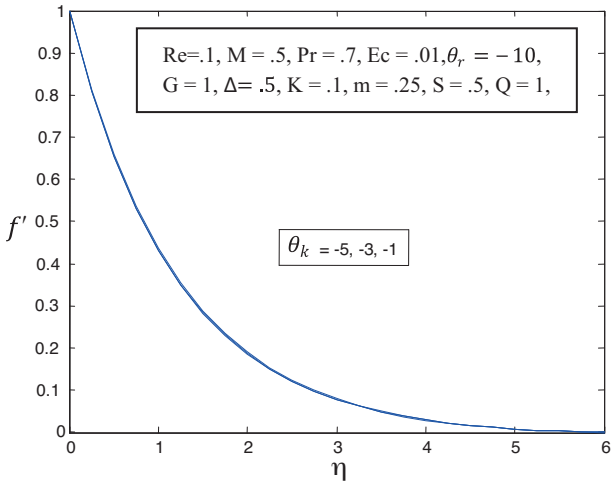

Figure 3. Velocity profile for different values of θ_k.

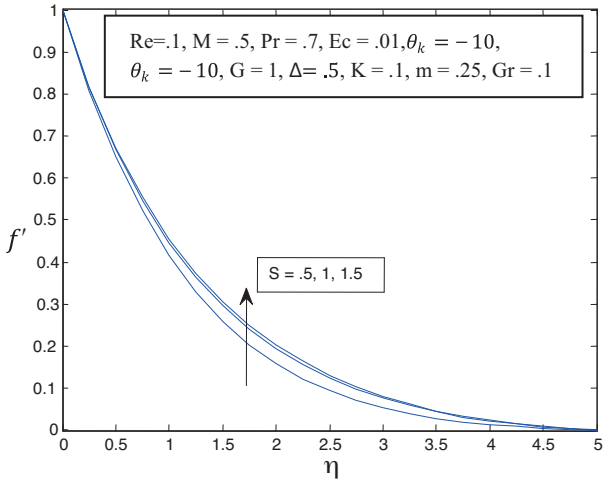

Figure 4. Velocity profile for different values of S.

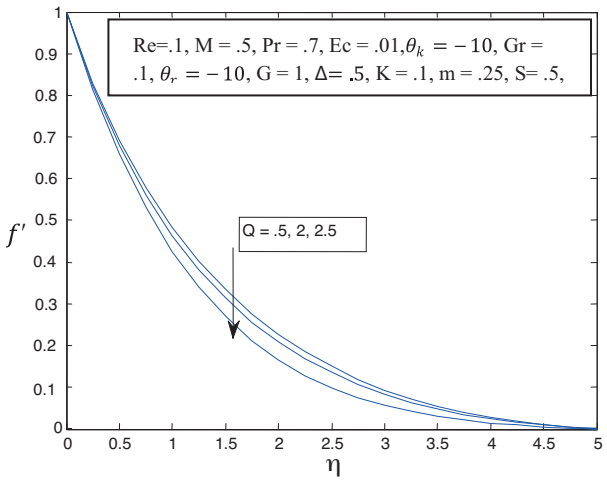

Figure 5. Velocity profile for different values of Q.

Figures 8–12 display the graphs obtained for the microrotation profile with the variations of θ_r, θ_k, Gr, G, and K. From Figures 8, 10, and 12 it is observed that microrotation increases with the increase of the viscosity parameter θ_r and the Grashof number Gr, i.e. due to the viscous and buoyancy force, microrotation increases, but it decreases with the increasing values of the coupling constant parameter K, where the variations

in microrotation are very significant near the plate. From Figure 11 it can be seen that microrotation decreases as the microrotation parameter G increases, while Figure 9 shows that microrotation does not change with the thermal conductivity parameter θ_k.

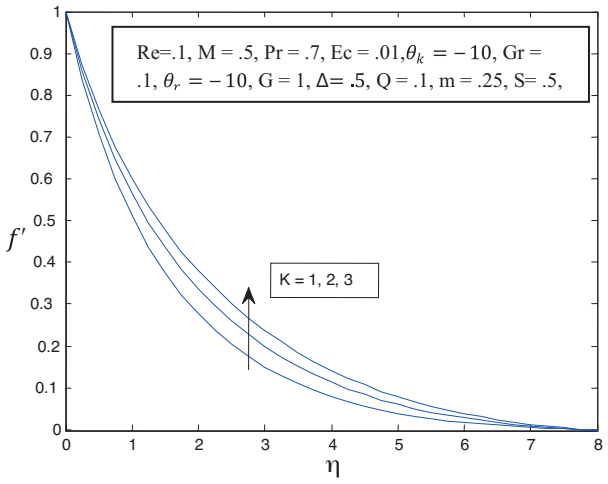

Figure 6. Velocity profile for different values of K.

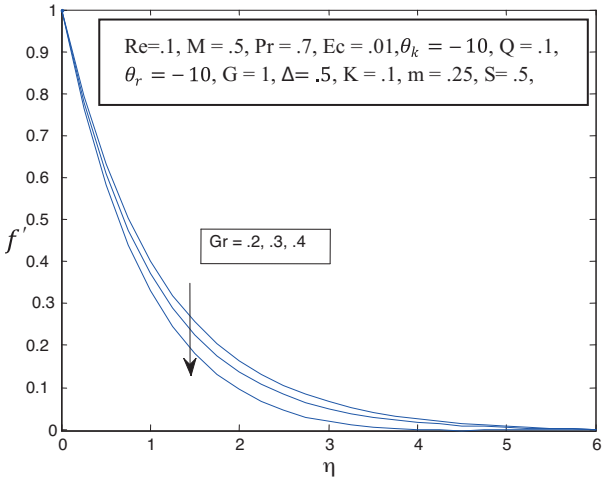

Figure 7. Velocity profile for different values of Gr.

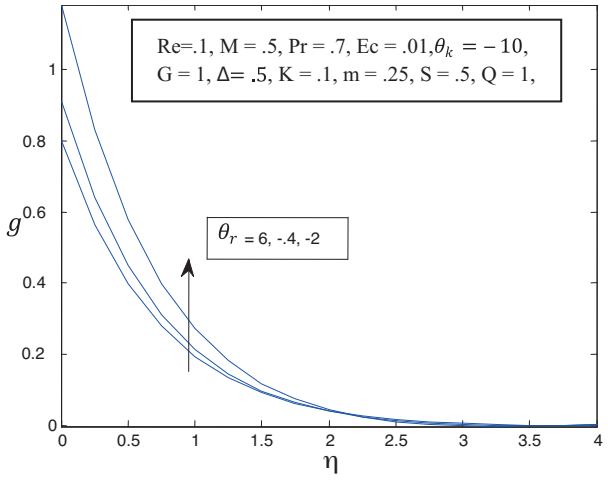

Figure 8. Micro-rotation profile for different values of θ_r.

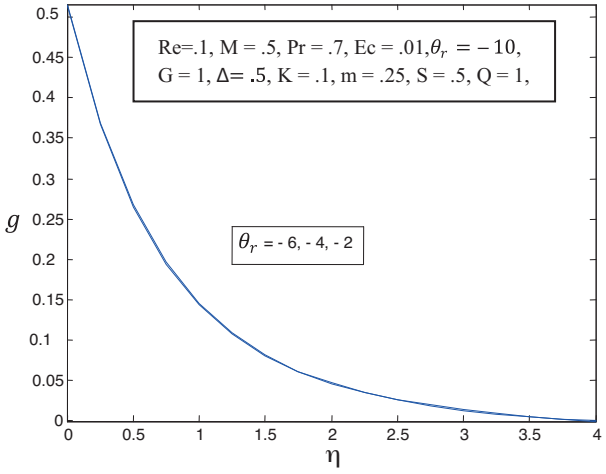

Figure 9. Micro-rotation profile for different values of θ_k.

The variations in the dimensionless temperature profile for various values of θ_r, θ_k, S, Q, and M are shown in Figures 13–17. It is seen from these Figures that temperature increases with the increase of the viscosity parameter θ_r, heat generation parameter Q, and Hartmann number M, whereas increasing values of the thermal conductivity parameter θ_k and the radiation parameter S reduce the temperature. This is due to the increase in viscous force and Lorentz force and the generation of heat during the flow, resulting in temperature increases; however, when thermal conductivity and radiation increase, temperature decreases.

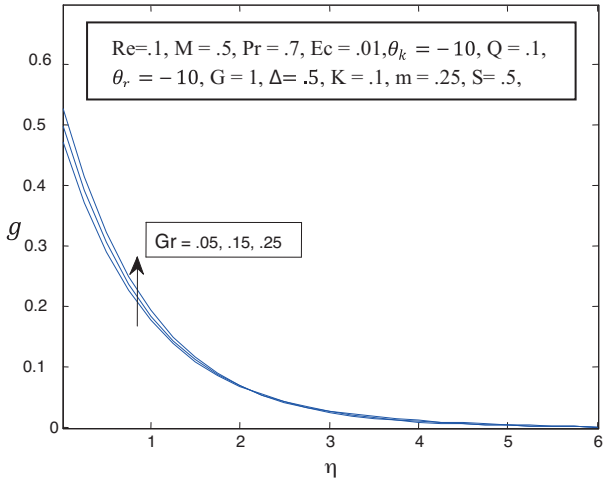

Figure 10. Micro-rotation profile for different values of Gr.

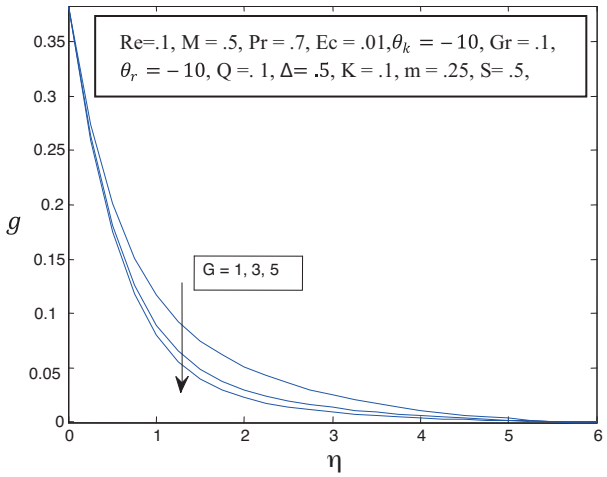

Figure 11. Micro-rotation profile for different values of G.

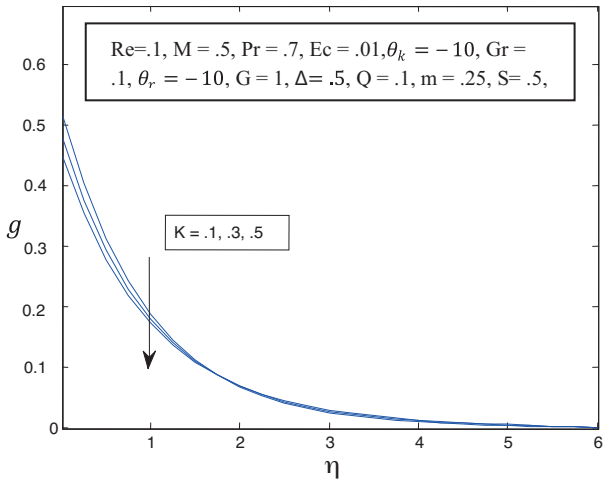

Figure 12. Micro-rotation profile for different values of K.

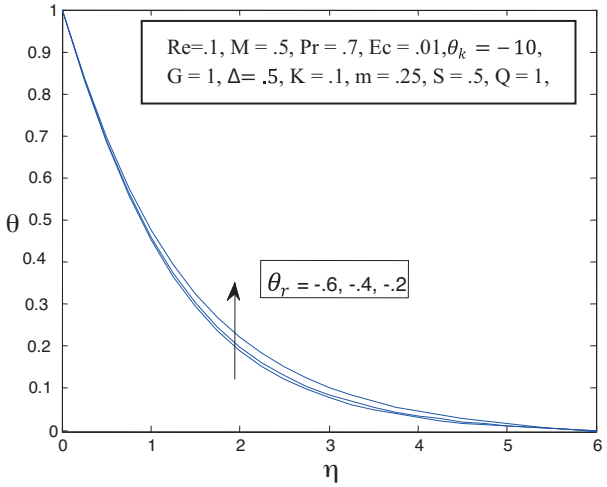

Figure 13. Temperature profile for different values of θ_r.

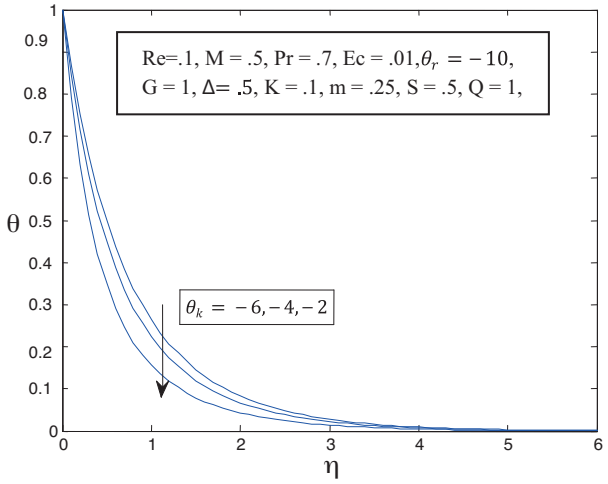

Figure 14. Temperature profile for different values of θ_k.

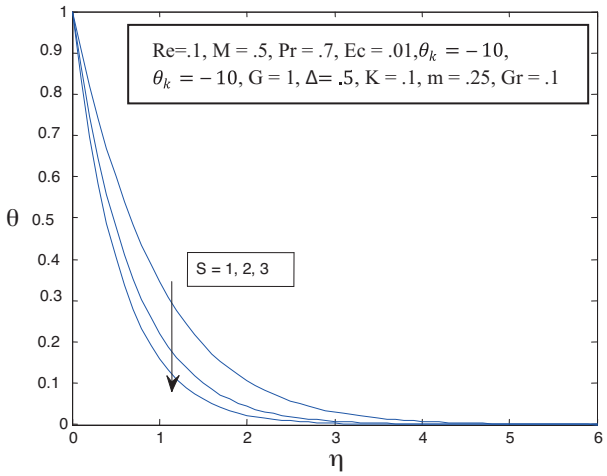

Figure 15. Temperature profile for different values of S.

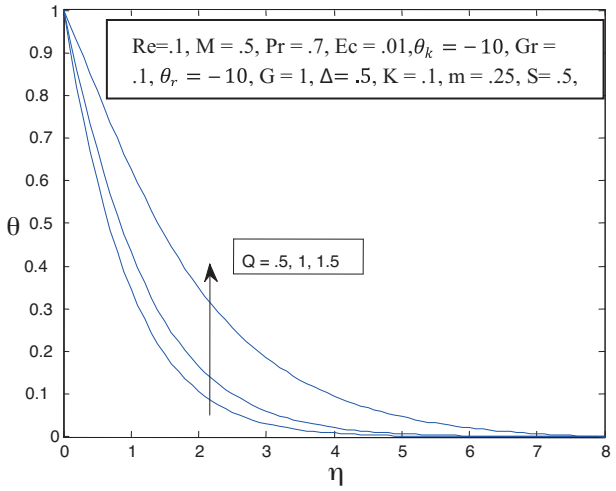

Figure 16. Temperature profile for different values of Q.

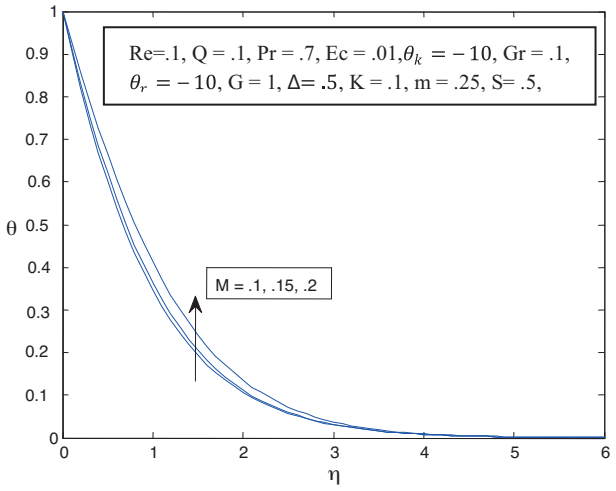

Figure 17. Temperature profile for different values of M.

The missing values $f''(0)$, $g'(0)$, $\theta'(0)$ and the coefficient of skin friction C_f , i.e. the wall shear stress and the Nusselt number Nu, which represents the heat transfer rate, are estimated for various combinations of parameters and displayed in Tables 1–4. From Table 1–4 it is seen that $f''(0)$, $g'(0)$, $\theta'(0)$, and C_f increase, whereas Nu decreases with the increase of Hartmann number M; however, for increasing values of θ_r, $f''(0)$, $g'(0)$ and Nu decrease, whereas $\theta'(0)$ and C_f are enhanced. From the same Tables we also found that $f''(0)$, $g'(0)$, and Nu increase and $\theta'(0)$ decreases with the increase of the coupling constant parameter K and θ_k , whereas C_f decreases with the increase of the coupling constant parameter K and increases with the increase of the thermal conductivity parameter θ_k.

Table 1. Missing values $f''(0)$, $g'(0)$, $\theta'(0)$ and values of the skin friction coefficient and Nusselt number for the values of Re = 0.1, Pr = 0.7, Ec = 0.01, $\theta_k = -10$, G = 1, $\Delta = 0.5$, K = 0.1, m = 0.25, S = 0.5, Q = 1, Gr = 0.1.

M	θ_r	$f''(0)$	$g'(0)$	$\theta'(0)$	cf	Nu
0.1	–10	–0.9575	–0.64866	–0.2408	–2.90402	0.069226
	–8	–0.96976	–0.65814	–0.23865	–2.87924	0.068607
	–6	–0.98973	–0.67356	–0.23513	–2.83919	0.067595
	–4	–1.02811	–0.70309	–0.22833	–2.7635	0.065639
	–2	–1.13251	–0.78277	–0.20961	–2.56662	0.060258
0.2	–10	–0.78108	–0.51458	–0.14929	–2.36895	0.042918
	–8	–0.79118	–0.52237	–0.1485	–2.34903	0.042691
	–6	–0.80765	–0.53507	–0.14719	–2.31686	0.042314
	–4	–0.83935	–0.55943	–0.14456	–2.25612	0.041557
	–2	–0.92592	–0.62557	–0.13669	–2.09841	0.039296
0.3	–10	–0.42388	–0.23464	0.116625	–1.2856	0.03353
	–8	–0.42905	–0.23834	0.115105	–1.27385	0.03309
	–6	–0.43745	–0.24438	0.112676	–1.25488	0.03239
	–4	–0.45358	–0.25596	0.108177	–1.21918	0.0311
	–2	–0.49733	–0.28745	0.096998	–1.1271	0.02789

Table 2. Missing values $f''(0)$, $g'(0)$, $\theta'(0)$ and values of the skin friction coefficient and Nusselt number for the values of Re = 0.1, Pr = 0.7, Ec = 0.01, $\theta_k = -10$, G = 1, $\Delta = 0.5$, M = 0.5, m = 0.25, S = 0.5, Q = 1, Gr = 0.1.

K	θ_r	$f''(0)$	$g'(0)$	$\theta'(0)$	cf	Nu
0.1	–10	–1.02078	–0.68302	–0.52325	–3.09594	0.150424
	–8	–1.03365	–0.69347	–0.52272	–3.06893	0.150272
	–6	–1.0546	–0.71046	–0.52187	–3.02528	0.150026
	–4	–1.09478	–0.74295	–0.52023	–2.94269	0.149554
	–2	–1.20346	–0.83028	–0.51582	–2.72739	0.148288
0.3	–10	–0.99262	–0.6615	–0.52413	–3.32443	0.150677
	–8	–1.00383	–0.67059	–0.52366	–3.29785	0.150542
	–6	–1.022	–0.68528	–0.5229	–3.25492	0.150324
	–4	–1.0565	–0.71311	–0.52146	–3.17389	0.149909
	–2	–1.1476	–0.78608	–0.51765	–2.96371	0.148813
0.5	–10	–0.96931	–0.64367	–0.52478	–3.55288	0.150863
	–8	–0.97923	–0.6517	–0.52436	–3.52668	0.150742
	–6	–0.99524	–0.66464	–0.52368	–3.48443	0.150547
	–4	–1.02544	–0.68896	–0.52239	–3.40485	0.150177
	–2	–1.10373	–0.75154	–0.51904	–3.19944	0.149213

Table 3. Missing values $f''(0)$, $g'(0)$, $\theta'(0)$ and values of the skin friction coefficient and Nusselt number for the values of Re = 0.1, Pr = 0.7, Ec = 0.01, $\theta_r = -10$, G = 1, $\Delta = 0.5$, K = 0.1, m = 0.25, S = 0.5, Q = 1, Gr = 0.1.

M	θ_k	$f''(0)$	$g'(0)$	$\theta'(0)$	cf	Nu
0.1	–10	–0.9575	–0.64866	–0.2408	–2.90402	0.069226
	–8	–0.95689	–0.64846	–0.25864	–2.90217	0.072702
	–6	–0.95613	–0.6482	–0.2772	–2.89986	0.075136
	–4	–0.95492	–0.64779	–0.30146	–2.8962	0.076265
	–2	–0.95205	–0.6468	–0.35579	–2.88748	0.077006
0.2	–10	–0.78108	–0.51458	–0.14929	–2.36895	0.042918
	–8	–0.77908	–0.51372	–0.21403	–2.36289	0.060162
	–6	–0.77717	–0.51289	–0.27051	–2.3571	0.073323
	–4	–0.77503	–0.51194	–0.3242	–2.35059	0.082016
	–2	–0.77125	–0.51026	–0.40226	–2.33912	0.084804
0.3	–10	–0.42388	–0.23464	0.116625	–1.2856	0.03353
	–8	–0.41721	–0.23064	–0.06762	–1.26535	0.049007
	–6	–0.41151	–0.2272	–0.22167	–1.24809	0.060084
	–4	–0.40654	–0.22418	–0.35051	–1.233	0.088672
	–2	–0.40088	–0.22072	–0.48491	–1.21583	0.102227

In order to assess the computed results, the present results have been compared with those obtained by Xenos [12], which are shown in Table 5. We found that our results agree very well with those reported by Xenos [12].

4. Conclusion

From the above investigations it is clear that the viscosity and thermal conductivity along with the other parameters such as the Hartmann number M, radiation parameter R, heat generation parameter Q, coupling constant parameter K, microrotation parameter G, and Grashof number Gr have significant effects on velocity, microrotation, and the temperature profile. The following conclusions can be drawn from this analysis:

Table 4. Missing values $f''(0)$, $g'(0)$, $\theta'(0)$ and values of the skin friction coefficient and Nusselt number for the values of Re = 0.1, Pr = 0.7, Ec = 0.01, $\theta_r = -10$, G = 1, $\Delta = 0.5$, M = 0.5, m = 0.25, S = 0.5, Q = 1, Gr = 0.1.

K	θ_k	$f''(0)$	$g'(0)$	$\theta'(0)$	cf	Nu
0.1	–10	–1.02078	–0.68302	–0.52325	–3.09594	0.150424
	–8	–1.02064	–0.68301	–0.54	–3.09552	0.15179
	–6	–1.02046	–0.68299	–0.5593	–3.09498	0.151598
	–4	–1.02017	–0.68296	–0.58764	–3.09409	0.148662
	–2	–1.01945	–0.68288	–0.65542	–3.09191	0.138174
0.3	–10	–0.99262	–0.6615	–0.52413	–3.32443	0.150677
	–8	–0.99249	–0.66148	–0.54109	–3.32399	0.152097
	–6	–0.99232	–0.66145	–0.56057	–3.32343	0.151945
	–4	–0.99205	–0.6614	–0.58911	–3.32251	0.149033
	–2	–0.99137	–0.66128	–0.65719	–3.32025	0.138547
0.5	–10	–0.96931	–0.64367	–0.52478	–3.55288	0.150863
	–8	–0.96919	–0.64364	–0.54192	–3.55242	0.152329
	–6	–0.96903	–0.6436	–0.56155	–3.55183	0.15221
	–4	–0.96877	–0.64355	–0.59024	–3.55089	0.14932
	–2	–0.96813	–0.6434	–0.65856	–3.54857	0.138836

Table 5. Comparisons of missing values $f''(0)$ and $\theta'(0)$ for the values of Re = 0.1, Pr = 0.7, Ec = 0.01, $\theta_r = -10$, G = 1, $\Delta = 0.5$, M = 0, m = 0.25, S = 0.5, Q = 1, Gr = 0.1.

Xenos [12] results				Present results	
Pr	θ_r	$f''(0)$	$\theta'(0)$	$f''(0)$	$\theta'(0)$
0.5	–10	–0.38378	–0.50795	–0.38373	0.50789
	–8	–0.3819	–0.50792	–0.3814	–0.5079
	–6	–0.37730	–0.50796	–0.37737	–0.50793
	–4	–0.36868	–0.50798	–0.36878	–0.50795
	–2	–0.34003	–0.50802	–0.34012	–0.50799
0.6	–10	–0.37259	–0.45439	–0.37268	–0.45431
	–8	–0.37098	–0.45442	–0.37007	–0.45433
	–6	–0.36548	–0.45445	–0.36559	–0.45436
	–4	–0.35607	–0.45451	–0.35616	–0.45447
	–2	–0.32520	–0.45469	–0.32531	–0.45464
0.7	–10	–0.36229	–0.40048	–0.36238	–0.40043
	–8	–0.35943	–0.40053	–0.35951	–0.40045
	–6	–0.35436	–0.40056	–0.3546	–0.4005
	–4	–0.34430	–0.40066	–0.34438	–0.40062
	–2	–0.32138	–0.40106	–0.32146	–0.40096

1. Thermal conductivity decreases the temperature, whereas viscosity increases it.
2. Viscosity reduces the velocity of the fluid, but enhances the microrotation of the fluid element.
3. The effect of temperature gets reduced due to radiation.
4. The effect of magnetic field enhances the temperature.
5. The effects of viscosity and thermal conductivity increase the wall shear stress; viscosity decreases the rate of heat transfer, while thermal conductivity increases it.

The results of the present study will be useful for the investigation of more complex MHD flow problems of micropolar fluid in different branches of science.

Nomenclature

ρ	fluid density,
μ	coefficient of dynamic viscosity,
T	fluid temperature,
λ	thermal conductivity,
m^*	coefficient of permeability,
j	microinertia per unit mass,
C_p	specific heat at constant pressure,
σ	electrical conductivity,
γ	material parameter,
κ	material parameter,
q_r	radiative heat flux,
g	acceleration due to gravity,
β	coefficient of thermal expansion,
Q_0	heat generation coefficient,
a^*	absorption coefficient,
σ^*	Stefan–Boltzmann constant,
Re	stretching Reynolds number,
G	microrotation parameter,
K	coupling constant parameter,
Δ	material constant,
M	Hartmann number,
m	permeability number,
Pr	Prandtl number,
Ec	Eckert number,
S	radiation parameter,
Q	heat generation parameter,
Gr	Grashof number.

References

[1] Eringen A.C. *Int. J. Eng. Sci.* **1964,** *2*, 205-217.

[2] Mohanty, B.; Mishra, S. R.; Pattanayak, H. B. *Alexandria Eng. J.* **2015**, *54*, 223-332.

[3] Si, X.; Zheng, L.; Zhang, X.; Chao, Y. *Appl. Math. Mech.-Engl. Ed.* **2010**, *31*, 1073-1080.

[4] Ashraf, M.; Batool, K. *J. Theor. Appl.* **2013**, *51*, 25-38.

[5] Si, X.; Zheng, L.; Lin, P.; Zhang, X.; Zhang, Y. *Int. J. Heat Mass Tran.* **2013**, *67*, 885-895.

[6] Raptis, A.; Perdikis, C. *Int. J. Appl. Mech. and Eng.* **2003**, *8*, 131-134.

[7] Siddheshwar P.G.; Mahabaleshwar U. S. *Int. J. Appl. Mech. and Eng.* **2015**, *20*, 397-406.

[8] Rahman, G. M. A. *J. Mod. Phys.* **2011**, *2*, 1290-1304.

[9] Khedr, M. E. M.; Chamkha, A. J.; Bayomi, M. *Nonlinear Anal.: Modelling and Control* **2009**, *14*, 27-40.

[10] Borgohain, B.; Hazarika, G. C. *Far East J. Appl. Math.* **2010**, *39*, 139-149.

[11] Raptis, A. *Therm. Sci.* **2011**, *15*, 849-857.

[12] Xenos, M. *Appl. Math.* **2013**, *4*, 1-5.

[13] Lai, F.C.; Kulacki, F.A. *Int. J. Heat Mass Tran.* **1990,** *33*,1028-1031.